J. Applied Membrane Science & Technology, Vol. 23, No. 3, December 2019, 65–74

Synthesis of GMA/EDMA Uniform Pores Monolith Using Melt blown Polypropylene Nanofibers Templates

Z. Kamin[a,c*], N. Ramon[b], M. Misson[d], C. C. Ken[a], R. Sarbatly[b], D. Krishnaiah[b] & A. Bono[b]

[a]Oil and Gas Engineering Programme, Faculty of Engineering, Universiti Malaysia Sabah, Jalan UMS, 88400, Kota Kinabalu, Sabah, Malaysia
[b]Chemical Engineering Programme, Faculty of Engineering, Universiti Malaysia Sabah, Jalan UMS, 88400, Kota Kinabalu, Sabah, Malaysia
[c]Energy Research Unit, Faculty of Engineering, Universiti Malaysia Sabah, Jalan UMS, 88400, Kota Kinabalu, Sabah, Malaysia
[d]Biotechnology Research Institute, Universiti Malaysia Sabah, Jalan UMS, 88400, Kota Kinabalu, Sabah, Malaysia

Submitted: 7/07/2019. Revised edition: 27/08/2019. Accepted: 31/08/2019. Available online: 20/09/2019

ABSTRACT

Glycidyl methacrylate/ethyl dimethacrylate (GMA/EDMA) monoliths consisting of pores induced by polypropylene nanofibers (PPNF) were developed. For creating these pores, templating technique was used where the PPNF act as a template. The PPNF were fabricated using a melt blowing technique at various process operations of polymer flowrate, air pressure and die-to-collector distance at ranges of 15 to 30 Hz, 0.15 to 0.3 MPa and 0.20 to 0.6 m respectively designed using a response surface methodology (RSM). Subsequently, a monolith solution was synthesis using the polymerization of GMA and EDMA, with azobisisobutyronitrile (AIBN) as initiator and cyclohexanol as porogen. The PPNF and GMA/EDMA monoliths were characterized using SEM and melting point instrument. The findings show, PPNF fiber diameter and melting points were in the range of 5 to 14×10^3 nm and 120 to 130 °C respectively. RSM analysis suggests that air pressure and die-to-collector distance could be an important factor for PPNF final diameter. Morphology studies demonstrate that GMA/EDMA monolith have been successfully acquired mesoporous structure and creating uniform pores by PPNF template produce at 22.5 Hz, 0.22 MPa and 0.40 m. As a conclusion, the PPNF can be proposed as a template to prepare monolith having uniform pores.

Keywords: Nanofiber, template, monolith, polypropylene, melt blown

1.0 INTRODUCTION

A monolith is a material consisting of connected pore channels. Monolith applications include as a separation media in gas adsorption [1], transport processes [2], water purification [3] and oil absorption [4]. Materials used to create monolith are metallic [5], ceramic [5] and carbon [6].

The techniques to produce monolith are free radical processes, polymerized high internal phase emulsions, cryogels, living polymerizations, soluble polymers and polycondensation [7].

One key property of monolith is its porous structure indicated by its pore sizes which make it suitable for the application of separation, catalysis and solid-phase chemistry [8].

Polymerization of Glycidyl methacrylate/ethyl dimethacrylate (GMA/EDMA) able to produce a

* Corresponding to: Z. Kamin (email: zykamilia@ums.edu.my)
DOI: https://doi.org/10.11113/amst.v23n3.165

porous structure within the monolith. This is achieved by tuning key parameters such as temperature, composition of the pore-forming solvent mixture, and content of cross-linking divinyl monomer [8]. Previous, preparation, characterization and functionalization of porous polymethacrylate monoliths have been extensively studied [7, 9–11].

However, the limitation faced during the monolith production is uneven pore distribution on the monolith structure leading to a "wall-channel" effect, causing internal pressure built up therefore reducing its efficiency and also a relatively low mechanical strength [12].

Alternative to the conventional porogen-based method, a template-based method able to precisely control the pore size, porosity, and interconnectivity of the monolith. This is done by incorporating nanoparticles template in a polymer matrix followed by template removal by dissolution or heating method (Ongkudon and Wong, 2014).

Guillemot *et al*. [13], fabricated a silica-based monolith by using poly(methyl methacrylate) nanoparticles as template. The template was then removed by pyrolysis at 480 °C for 48 hrs. Klepel *et al*., [14] using template method produced carbon/silica composite porous monolith after carbonization at 160 °C and calcination at 800 °C. The disadvantage of template-based silica monolith is the longer time needed for the formation of silica and the exclusion of the template.

Nanofiber has unique physical and mechanical properties, high surface area and small pores sizes making them suitable for various application [14–16].

Since to the best of our knowledge, only limited studies have been carried out on the templating using nanofiber, the objective of this study is to produce melt blown nanofibers with properties suitable to become a template to produce monolith with uniform pores.

2.0 METHODOLOGY

2.1 Design of Experiment by Central Composite Design (CCD)

The experimental design of the operating condition was performed using Response Surface Methodology (RSM) as used in other studies [17, 18]. The factors involves were, the polymer flowrate (Hz), air pressure (MPa) and die-to-collector distance (m) and were set in the ranges of 15 to 30 Hz, 0.15 to 0.3 MPa and 0.20 to 0.6 m respectively as shown in Table 1.

Table 1 Experiment design by CCD of RSM

Run	Air Pressure (MPa)	Polymer melt flow rate (Hz)	Die to collector distance (m)
1	0.23	22.50	0.40
2	0.15	30.00	0.60
3	0.23	22.50	0.40
4	0.23	35.11	0.40
5	0.23	22.50	0.40
6	0.30	15.00	0.20
7	0.23	22.50	0.06
8	0.35	22.50	0.40
9	0.23	22.50	0.74
10	0.30	15.00	0.60
11	0.23	22.50	0.40
12	0.15	15.00	0.60
13	0.23	9.89	0.40
14	0.15	30.00	0.20
15	0.23	22.50	0.40
16	0.30	30.00	0.60
17	0.10	22.50	0.40
18	0.23	22.50	0.40
19	0.15	15.00	0.20
20	0.30	30.00	0.20

2.2 Production of PPNF using Melt Blowing Technique

The melt blowing technique was used to produce the PPNF. Polypropylene (Sun Allomer) was supplied into the extruder and heated gradually from room temperature to 300 °C to prevent polymer degradation meanwhile the air temperature was set at 450 °C. The manipulated variable were set to match the experimental design by Response Surface Methodology.

2.3 Preparation of Monolith Solution

A 5 ml solution containing 60 % of porogen and 1 % of mixture of Azobisisobutyronitrile (AIBN), cyclohexanol, glycidyl methacrylate (GMA) and ethyl dimethacrylate (EDMA) were used for the monolith fabrication. The mixture contains 20 mg of AIBN, 1.4 ml of GMA, 0.6 ml of EDMA and 3 ml of porogen.

2.4 Incorporation of Monolith-PPNF

100 mg of PPNFs was soaked into the monolith solution and put into an ultrasonicator for 20 mins at 28 ˚C. It then heat treated at 60 ˚C for 90 mins in a water bath. Next, the PPNF-monolith was soaked with methanol and leave for overnight, before being washed using distilled water. The structure was then sintered using Furnace (46100, High Temperature Furnace, Thermolyne) at 150˚C for 30 minutes.

2.5 Characterization Techniques

Scanning Electron Microscope (S-3400N, Hitachi, Japan) was used to obtain the average diameter of the PPNF and monoliths. The melting point of PPNF was analyzed by a Melting Point Instrument (MP, HISBY) to study any change in melting point due to the thermal treatment by the melt blowing process and to select the lowest sintering temperature for fiber removal. Homogeneity of PPNF was analyzed by calculating the standard deviation of the PPNFs diameters.

3.0 RESULTS AND DISCUSSION

3.1 Physical Observation of the PPNF

As shown in Figure 1, Sample 2, 4, 6, 7, 14, 15, 19 and 20 show the occurrence of fuse fibers to a certain degree, therefore forming an underdeveloped fiber web. This is due to the incomplete separation of individual fibers which is influenced by the melt blowing operating conditions. These fibers were undesirable to be used as a PPNF monolith template.

Samples 1, 3, 5, 8, 9, 12, 16 and 17 shows the formation of crystal inside the fiber web indicated by the occurrence of small bead particles. This may due to the incomplete melting of the PP polymers which related to the polymer melt flow rate. Some of the fiber also shown fused fibers to a certain degree. These fibers were also excluded as the PPNF monolith template.

Subsequently, for Samples 10, 11, 13, and 18, although these samples are showing some fused fibers there were no crystal formed on the PPNF which is a characteristic that is desired for a monolith template.

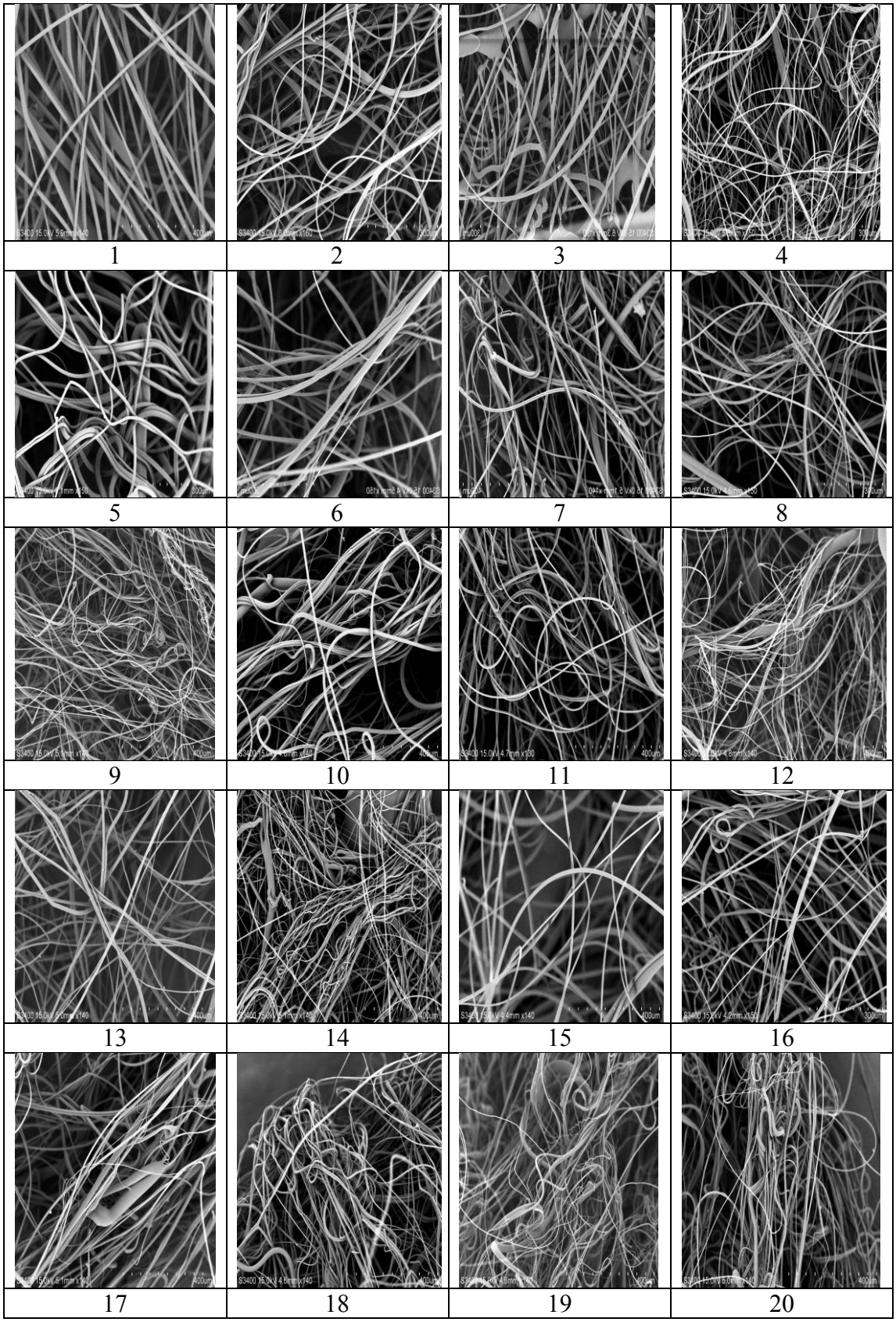

Figure 1 SEM images of the PP fibers samples spun at operating conditions stated in Table 1

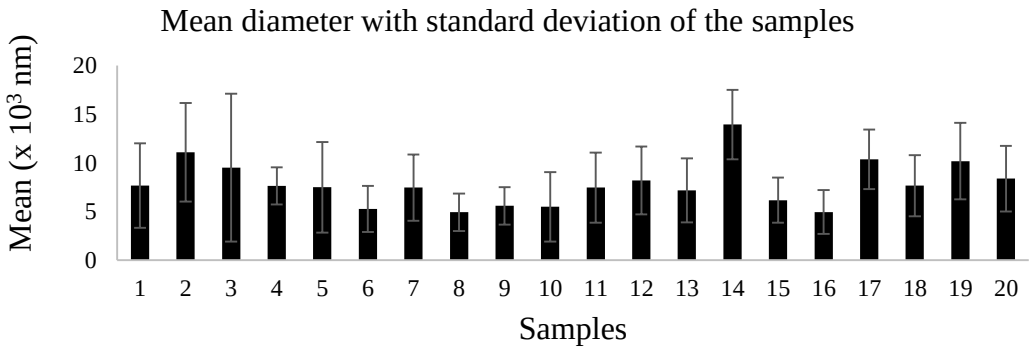

Figure 2 Mean diameter with standard deviation of the melt-blowing PP fiber samples spun at operating conditions stated in Table 1

3.2 Diameter of the PPNFs

Figure 2 shows the mean diameters with standard deviation of the samples. The average PPNFs diameters observed from SEM were in the range of 4.94 to 13.95 × 10^3 nm, which are slightly higher [19–21] but comparable [22] to other studies.

At a constant polymer flowrate and die-to-collector distance, Sample 10 conditioned at a higher pressure than Sample 12 acquired smaller average diameter of 5.5 × 10^3 nm in contrast to 8.21 × 10^3 nm. Here, there is enough force for the attenuation process to occur and to overcome the drag force to produce fibers with smaller sizes. The average diameter of a fiber can decrease in sizes as the air pressure is increased [23].

Sample 11 which conditioned at a higher polymer flowrate than Sample 13 produce larger average fiber diameter of 7.47 19 × 10^3 nm in opposed to the later at 7.19 × 10^3 nm. An increase in the polymer flowrate, decrease the drag force acting on the polymer filament therefore increase the size of fiber diameter [19].

Sample 9 having die-to-collector distance of 74 cm was found to have a smaller average fiber diameter of 5.59 × 10^3 nm than Sample 11 which having die-to-collector of 40 cm having an average diameter of 7.47× 10^3 nm.

As the distance of fiber collector increases the average fiber diameter decreases [24]. This length provides enough time for the attenuation process to occur on the fiber filament therefore decreases fiber size.

The standard deviations of the average fiber diameters were found to be majority in between 1 and 3. Sample 4 and Sample 3 show the lowest and highest standard deviations at 1.91 and 7.6 respectively. A high standard deviation indicates inhomogeneous PPNF.

3.3 RSM Analysis

ANOVA evaluation indicated that the model obtained is significant. The regression model in actual term for average fiber diameter D is:

$$D = +10.03892A + 0.30732B + 4.04331C - 0.90444AB + 13.58333AC - 0.37750BC + 46.99563A^2 + 3.22250E\text{-}003B^2 - 3.37912C^2 \quad (1)$$

where A is air pressure, B is polymer flow rate and C is the die-to-collector distance.

The Model F- value of 5.09 implies the model is significant with a p value at 0.009. The term model in this case, A and C are significant as the p values are less than 0.0500 i.e. 0.0002 and 0.0478 respectively. However, for B,

the p value is 0.0712, which is lesser than 0.1000 in which model term greater than this value is considered not significant. The model graph shows that as both of the air pressure and die-to-collector distance increase, the average fiber diameter decrease, with air pressure was shown to have a more significant impact.

Table 2 Process parameter used for nanofiber fabrication as monolith template

Samples	Air pressure (MPa)	Polymer Flowrate (Hz)	Die to collector distance (m)	Average diameter (x 10^3 nm)	Standard deviation	Melting point ^oC
A	0.22	9.89	0.40	5.50	3.57	123.8
B	0.30	15.00	0.60	7.47	3.60	125.7
C	0.22	22.50	0.40	7.19	3.29	127.7

Therefore, this finding indicates that air pressure and die-to-collector distance are significant model terms in influencing the average diameter of the PPNF for the studied ranges.

3.4 Melting Point of PPNF

The melting point of the PPNFs was in the range of 120 to 130 ˚C whereas PP granules used for PPNF fabrication were 138 ˚C.

This means that there is no significant change occurred in PPNF properties after sintering. The melting point of the PPNF was analyzed to select the temperature for PPNF removal in order to produce GMA/EDMA monolith.

3.5 Monolith Template Selection

PPNF templates were selected based on (1) there is no crystallized formed inside the fiber web, (2) the average fiber diameter is not too small. The melting points were not considered as there are insignificant changes after processing, therefore is not considered. These criteria are required to ensure that the PPNF template able to produce uniform pores and removable from the PPNF-monolith structure.

The PPNF having crystal beads will cause uneven pores sizes distribution inside the monolith structure and difficult to remove from the monolith. In which, Sample 10, 11, 13 and 18 fit criteria (1). However, since Sample 10 and 8 has a same process condition, only Sample 10 was selected.

For the average fiber diameter, it is important to choose not too small average fiber diameter due to the difficulty for flushing out the melted PPNF from the monolith structure during the sintering process. The overall average fiber diameter was appropriate since the aim was not to use fibers with too small average fiber diameter.

Sample 10, 11, 13 have an average diameter of 5.50, 7.47 and 7.19 × 10^3 nm. Therefore, Sample 10, 11 and 13 was chosen as the template for monolith preparation. The process parameters used to condition Sample 10, 11 and 13 are shown in Table 2 and later denoted as A, B and C.

3.6 PPNF-Monolith Observation and Characterization

3.6.1 Physical Observation of PPNF – Monolith Preparation

The structure of the PPNF and monolith before and after sintering in a furnace at 130 ˚C for 30 minutes are shown in Figure 3. After sintering, the

top of the monolith structure shows cracks. This may due to the heat produced from the melted PPNFs. Additionally, the melted PPNFs may not able to be fully flushed out from the monolith structure causing it to remain in the structure as clogs.

In addition, Samples A and B break into two after sintering, which indicates that they are very fragile compared to Sample C. Sample C was hard and retained its solid structure after sintering. This might be due to the PPNF distribution in monolith solution. The PPNF may not be completely soaked in the monolith solution since the PPNFs has chemical resistance to a certain degree, causing it to unevenly distributed inside the monolith solution [23] therefore having effect on its mechanical strength.

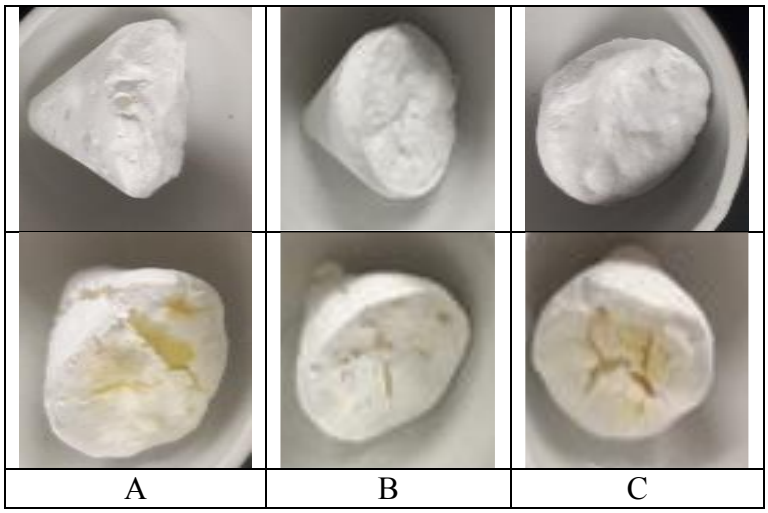

Figure 3 Nanofiber-monolith samples before sintering (top) and after sintering (bottom)

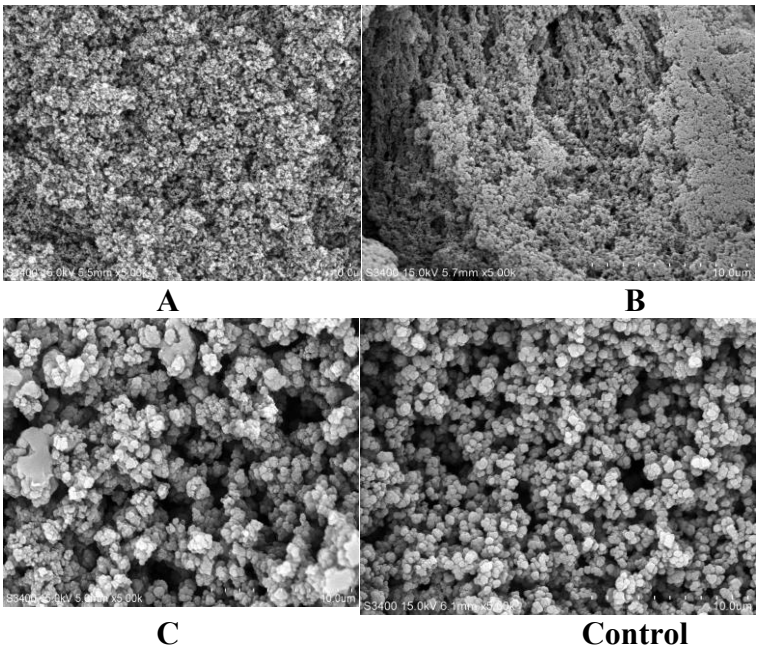

Figure 4 SEM images for samples of monolith for Sample A-C and control sample after the sintering process

3.6.2 Morphological Study of PPNF – Monolith by SEM

A morphological study on the GMA/EDMA monolith for Sample A shown in Figure 4 (A) indicates that the pore distribution is difficult to see as no pores was formed or the pores are too small compared to the control sample in Figure 4 (C) where the pores are clear and detectable.

Similarly, for Sample B, shown in Figure 4 (B) the pore distribution was difficult to notice as the pores are too small and the arrangement of particles is more compact compared to Sample A, C and control as shown in Figure 4. This may due to there was no reaction take place during the sintering process.

A normal pore morphology of polymethacrylate monoliths is characterized by interconnected globules that are partly aggregated [25] as shown in the control sample.

The structure of Sample C is almost similar to the control sample. However, some solid chunks of PP occurred at various points of the monolith, which may due also to the PP melt was unable to flow out through the monolith structure during the sintering process. Here a higher sintering temperature may be required to totally flush out the PP melt during the sintering process or a longer sintering time may be applied.

It can be said that Sample C is more likely formed pores in the monolith structure compared other Sample A and B. Moreover, Sample C is more rigid in structure where the other two are more fragile. Therefore, Sample C is suitable as a template for the monolith.

4.0 CONCLUSION

Melt blowing technique was used to produce PPNF by tuning the process parameter such as air pressure, polymer flowrate and die-to-collector distance in the ranges of 0.15 to 0.3 MPa, 15 to 30 Hz and 0.2 to 0.6 m respectively. The PPNF average fiber diameter obtained were in the range of 5 to 14 $\times$ 10^3 nm with melting points were in the range of 120 ˚C to 130 ˚C. PPNF conditioned at 0.22 MPa; 22.5 Hz and 0.4 m show the potential as a template for the fabrication of the monolith with uniform pores.

ACKNOWLEDGEMENT

This work was supported by the Ministry of Higher Education under the Fundamental Research Grant Scheme (FRGS) number FRGS0465-2017.

REFERENCES

[1] Couck, S., J. Cousin-saint-remi, S. Van Der Perre, G. V Baron, C. Minas, P. Ruch and J.F.M. Denayer. 2018. Microporous and Mesoporous Materials 3D-Printed SAPO-34 Monoliths for Gas Separation 1. *Microporous and Mesoporous Materials*. 255: 185-191.

[2] Grebenyuk, Y., H. X. Zhang, M. Wilhelm, K. Rezwan and M. E. Dreyer. 2017. Journal of the European Ceramic Society Wicking into Porous Polymer-Derived Ceramic Monoliths Fabricated by Freeze-Casting 1. *Journal of the European Ceramic Society*. 37(5): 1993-2000.

[3] Lin, P., L. Meng, Y. Huang and L. Liu. 2016. Colloids and Surfaces A : Physicochemical and Engineering Aspects Synthesis of Porous Polyurea Monoliths Assisted by

Centrifugation as Adsorbents for Water Purification. *Colloids and Surfaces A: Physicochemical and Engineering Aspects*. 506: 87-95.

[4] Wang, L., F. Ai, Y. Liu and Y. Liu. 2018. Porous Polyamide Monolith by Continuous Solution Foaming as Reusable Oils Aand Organic Solvents Absorbent. *Materials Letters*. 213: 44-47.

[5] Avila, P., M. Montes and E. E. Mir. 2005. Monolithic Reactors for Environmental Applications A Review on Preparation Technologies. *Chemical Engineering Journal*. 109(2005): 11-36

[6] Taubert, M., J. Beckmann, A. Lange, D. Enke and O. Klepel. 2014. Attempts to Design Porous Carbon Monoliths using Porous Concrete as a Template. *Microporous and Mesoporous Materials*. 197: 58-62.

[7] Svec, F. 2010. Porous Polymer Monoliths: Amazingly Wide Variety of Techniques Enabling Their Preparation. *Journal of Chromatography A*. 1217(6): 902-924.

[8] Viklund, C., F. Svec, J. M. J. Fréchet and K. Irgum. 1996. Monolithic, "Molded", Porous Materials with High Flow Characteristics for Separations, Catalysis, or Solid-phase Chemistry: Control of Porous Properties during Polymerization. *Chemistry of Materials*. 8(3): 744-750.

[9] Vlakh, E. G. and T. B. Tennikova. 2007. Preparation of Methacrylate Monoliths. *Journal of Separation Science*. 30(17): 2801-2813.

[10] Namera, A., A. Nakamoto, T. Saito and S. Miyazaki. 2011. Monolith As A New Sample Preparation Material: Recent Devices and Applications. *Journal of Separation Science*. 34(8): 901-924.

[11] Nischang, I. 2013. Porous Polymer Monoliths: Morphology, Porous Properties, Polymer Nanoscale Gel Structure and Their Impact on Chromatographic Performance. *Journal of Chromatography A*. 1287: 39-58.

[12] Ongkudon, C. M. and C. Wong. 2014. Challenges and Strategies in the Preparation of Large-volume Polymer-based Monolithic Chromatography Adsorbents. *Journal of Sep*. 37: 455-464.

[13] Guillemot, F., A. Brunet-bruneau, E. Bourgeat-lami, J. Boilot, E. Barthel and T. Gacoin. 2013. Percolation Transition in the Porous Structure of Latex-templated Silica Monoliths. *Microporous and Mesoporous Materials*. 172: 146-150.

[14] Reneker, D. H. and I. Chun, 1996. Nanometre Diameter Fibres Of Polymer, Produced by Electrospinning. *Nanotechnology*. 7(3): 216-223.

[15] Wu, J., N. Wang, Y. Zhao and L. Jiang. 2013. Electrospinning of Multilevel Structured Functional Micro-/Nanofibers and Their Applications. *Journal of Materials Chemistry A*. 1(25): 7290.

[16] Sarbatly, R., D. Krishnaiah and Z. Kamin. 2016. A Review of Polymer Nanofibres by Electrospinning and Their Application in Oil-water Separation for Cleaning Up Marine Oil Spills. *Marine Pollution Bulletin*. 106(1-2): 8-16.

[17] Kamin, Z., A. Bono and L.Y. Leong. 2017. Simulation and Optimization of the Utilization of

Triethylene Glycol in a Natural Gas Dehydration Process. *Chemical Product and Process Modeling*. 12(4).

[18] Bono, A., S. M. Anisuzzaman and O.W. Ding. 2014. Effect of Process Conditions on the Gel Viscosity and Gel Strength of Semi-refined Carrageenan (SRC) Produced from Seaweed (Kappaphycus Alvarezii). *Journal of King Saud University - Engineering Sciences*. 26(1): 3-9.

[19] Hassan, M. A., B. Y. Yeom, A. Wilkie, B. Pourdeyhimi and S. A. Khan. 2013. Fabrication of Nanofiber Meltblown Membranes and Their Filtration Properties1. *Journal of Membrane Science*. 427: 336-344.

[20] Ellison, C. J., A. Phatak, D. W. Giles, C. W. Macosko and F. S. Bates. 2007. Melt Blown Nanofibers: Fiber Diameter Distributions and Onset of Fiber Breakup. *Polymer*. 48(11): 3306-3316.

[21] Uppal, R., G. Bhat, C. Eash and K. Akato. 2013. Meltblown Nanofiber Media for Enhanced Quality Factor. *Fibers and Polymers*. 14(4): 660-668.

[22] Tan, D. H., C. Zhou, C. J. Ellison, S. Kumar, C. W. Macosko and F. S. Bates. 2010. Meltblown Fibers: Influence of Viscosity and Elasticity on Diameter Distribution. *Journal of Non-Newtonian Fluid Mechanics*. 165(15-16): 892-900.

[23] Safranski, D. L., J. M. Boothby, C. N. Kelly, K. Beatty, N. Lakhera, C. P. Frick, A. Lin, R. E. Guldberg and J. C. Griffis. 2016. Thermo-mechanical Behavior and Structure of Melt Blown Shape-memory Polyurethane Nonwovens. *Journal of the Mechanical Behavior of Biomedical Materials*. 62: 545-555.

[24] Versus, M. E., n.d. Polypropylene Nanofibers.

[25] Chan, Y. W., T. Kansil and C. M. Ongkudon. 2017. Analytical and Preparative Polymethacrylate Monolith Fabrication : Effect of Porogen Content and Column Size on Pore Morphology. *Colloid and Polymer Science.* 295(12): 2373-2382.